Nuclear Engineering and Design 415 (2023) 112616

Contents lists available at ScienceDirect

Nuclear Engineering and Design

journal homepage: www.elsevier.com/locate/nucengdes

Evaluation of the influence of the viscous sublayer on the mechanical stability of fuel plates under axial flow conditions

A.J.S. Moura [a,*], M. Mattar Neto [b]

[a] Navy Technological Center in Sao Paulo (CTMSP), Av. Professor Lineu Prestes, 2468, 05508-000 São Paulo, SP, Brazil
[b] Energy and Nuclear Research Institute (IPEN- CNEN), Av. Professor Lineu Prestes, 2242, 05508-000 São Paulo, SP, Brazil

ARTICLE INFO

Keywords:
Plate-type fuel element
Critical velocity
FSI
CFD
FEA

ABSTRACT

The current work aims to investigate the influence of the viscous sublayer on the mechanical stability of fuel element plates under axial flow conditions by means of two-way Fluid Structure Interaction (FSI) numerical simulations. The methodology adopted is that proposed by (Mantecón, 2019; Mantecón and Mattar Neto, 2018), who observed a transition from linear to non-linear behavior between the maximum deflection of the plates in their leading edge with the square of the velocity of the cooling fluid in the channel. The speed at which the transition is identified is the critical speed (V_c). In order to verify the influence of the viscous effects, the CFD domain was discretized from its viscous sublayer. As this approach greatly increases the computational cost, where the characteristics of the flow allowed, symmetry boundary conditions were used. In addition to this approach, it was decided to investigate the ability to solve the FSI problem in steady state. The obtained results confirmed that the boundary layer modeling is sufficient to determine the critical velocity. Furthermore, they also suggest that the steady-state approach and the application of symmetry boundary conditions, where possible, can be used in the design of new fuel elements, supporting traditional methods.

1. Introduction

Plate-type fuel elements (FE) are widely used in research reactors, with the main objectives of providing services and developing technology, such as: production of medical and industrial radioisotopes, testing of nuclear materials and fuels for power reactors, use of neutron beams for scientific and technological research in different fields of science, analysis by neutron activation, production of tracers for application in research in agriculture and the environment, and training of labor to work in the nuclear area, among others. Furthermore, it is also possible to find this type of FE in naval power reactors of the PWR type ("Pressurized Water Reactor"), presenting several advantages from the functional point of view when shipped and used in naval propulsion plants (de Sa Andrzejewski, 2005; Kaufmann, 1962).

Plate-type fuel elements (FE) consist of parallel plates containing nuclear fuel and separated by narrow channels, through which coolant flows to remove the heat generated by nuclear fission passes. The design of these FEs involves several trade-offs to meet requirements, such as being sufficiently thin so to avoid internal overheating, and resistant enough to maintain stability in the face of the high flows of coolant required for cooling. One of the main challenges in this project is dealing with the probability of the occurrence of structural instabilities due to hydrodynamic forces during operation (R. Doan The Engineering Test Reactor – A Status Report. 16, 1958; El-Wakil, 1962; Glasstone and Sesonske, 2012).

This flow-induced deflection in a plate-type assembly was reported in the literature for the first time by Stromquist and Sisman (Stromquist and Sisman, 1948) who verified experimentally that, when raising the coolant velocity to sufficiently high values, the fuel plates deformed plastically. In 1958, Ronald Doan (R. Doan The Engineering Test Reactor – A Status Report. 16, 1958) identified the same phenomenon during the design, development, and construction of the fuel element destined to be used in the Engineering Test Reactor (ETR). Doan qualitatively addressed the existence of a critical flow that would be related to the beginning of the plastic deformation of the plates.

Still in 1958, Daniel Miller (Miller, 1958) used Doan's theory and proposed the first analytical expression to calculate the critical flow velocity that would cause collapse in fuel element plates. His work was extremely relevant, as it resulted in the most widely used expression for calculating critical velocity. For this reason, many authors denote the critical flow velocity as "Miller Velocity". Equation (1) presents Miller's theoretical expression for predicting the critical flow velocity in a flat

* Corresponding author at: Av. Prof. Lineu Prestes, 2242 – Cidade Universitária, São Paulo. CEP:, 05508-000, São Paulo, Brazil.
E-mail addresses: alceumoura@usp.br (A.J.S. Moura), mmattar@ipen.br (M. Mattar Neto).

https://doi.org/10.1016/j.nucengdes.2023.112616
Received 15 July 2023; Received in revised form 16 September 2023; Accepted 18 September 2023
Available online 12 October 2023

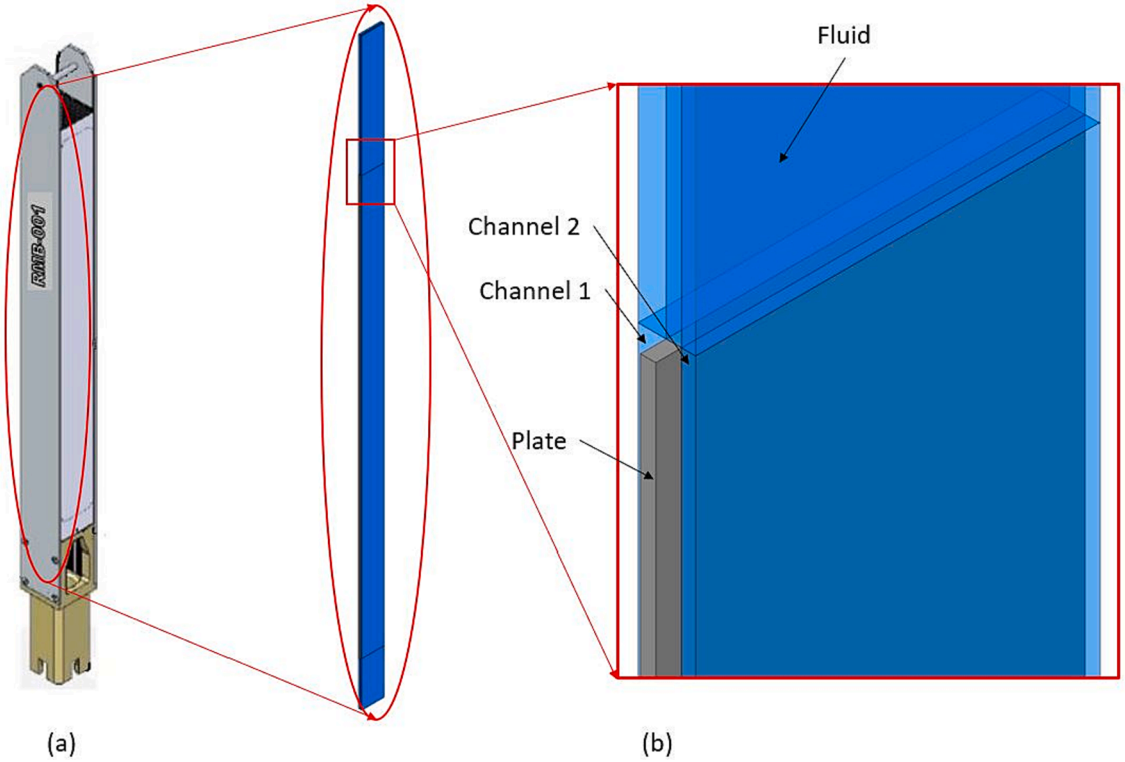

Fig. 1. (a) Isometric view and (b) multiphysics domain.

plate fuel assembly, where each plate has two edges attached and the other two are considered free:

$$V_M = \sqrt{\frac{15Ea^3h}{\rho b^4(1-\nu^2)}} \tag{1}$$

where: V_M = Miller's critical velocity; E = Young's modulus of elasticity; a = plate thickness; h = thickness of the channel; ρ = fluid density; b = channel width; ν = Poisson's ratio.

Until recently, analytical and experimental techniques were the only methods to quantify and address the impact of how reactor flows structurally affect fuel elements (Cekirge and Ural, 1978; Davis and Kim, 1991; Davis and Scarton, 1985; Groninger and Kane, 1963; Guo and Païdoussis, (03 2000),; Howard et al., 2015; Jensen and Marcum, 2014; Jensen, 2013; Johansson, 1959; Kim and Davis, 1995; Li et al., 2012; Pavone and Scarton, 1983; Scavuzzo, 1965; Smissaert, 1968; Smissaert, 1969; R.L. Smith Dynamic Pressure Limits for Flat Plates as Related to Nuclear Fuel Elements, 1968; Swinson et al., 1995; Swinson and Yahr, 1990; Wambsganss, 1967; Weaver and Unny, (09 1970)). At this point, it is worth a digression to point out a remarkable discovery: at the critical velocity predicted by Miller, the fuel element plates become statically unstable; and vibration is predicted for higher speeds, at approximately twice the Miller speed (Davis and Kim, 1991; Kim and Davis, 1995; Smissaert, 1968; Smissaert, 1969; Weaver and Unny, (09 1970)). However, with advances in computational time, numerical methods have become increasingly widely used and constitute the state of the art in the study of hydromechanical stability of fuel elements with the most diverse geometries. Thus, due to advances in computational power, several researchers have carried out studies of Fluid-Structure Interaction (FSI), coupling commercial codes of Computational Fluid Dynamics (CFD) and the Finite Element Method (Finite Element Analysis - FEA) to study flow-induced deflections in fuel elements (Curtis et al., 2013; Curtis et al., 2018; Curtis et al., 2019; Jesse, 2015; Kennedy, 2012; Kennedy, 2015; Mantecón, 2019; Mantecón and Mattar Neto, 2018; Mantecón and Mattar Neto, 2019; González Mantecón and Mattar Neto, 2020; Wang et al., 2023; Wang et al., 2023).

However, after an in-depth search, we found that in all analyses reported in the literature, researchers used turbulence models and mesh discretization that model the boundary layer, using the law of the wall. Thus, the main objective of the current work, based on the numerical methodology presented by Javier Mantecón (Mantecón, 2019; Mantecón and Mattar Neto, 2018), is to discretize the boundary layer from this viscous sublayer, to verify its contribution to the onset of mechanical instability of fuel plates in fluid–structure interaction simulations. In addition to the more refined treatment of the boundary layer, the current work differs from others already published by the use of symmetry boundary conditions, in order to capture the effect of contiguous plates with a less computational effort, in addition to performing the two-way fluid–structure analyses in steady state. Steady-state two-way FSI couplings have been employed in several areas, such as (Bang et al., 2022).

Finally, it can be observed that the research presented here has a direct connection to nuclear reactor technology, specifically those utilizing flat plate fuel elements. This connection can be divided into several aspects:

- Development and Improvement of Nuclear Reactors: The research addresses a critical issue related to the mechanical stability of fuel elements in nuclear reactors that use flat plate fuel elements. The mechanical instability of these elements can lead to serious problems, affecting the safety and operation of reactors. Therefore, the methodology discussed here can be applied to contribute to the development and improvement of nuclear reactors.
- Computational Fluid Dynamics (CFD) Studies: The research employs numerical simulations of fluid–structure interaction (FSI). This approach is essential for understanding how high fluid flow affects plate stability, which is crucial for optimizing the design of fuel elements and ensuring the safe operation of nuclear reactors. It can also explore how manufacturing deviations and reactor condition variations affect the behavior of the fuel element.

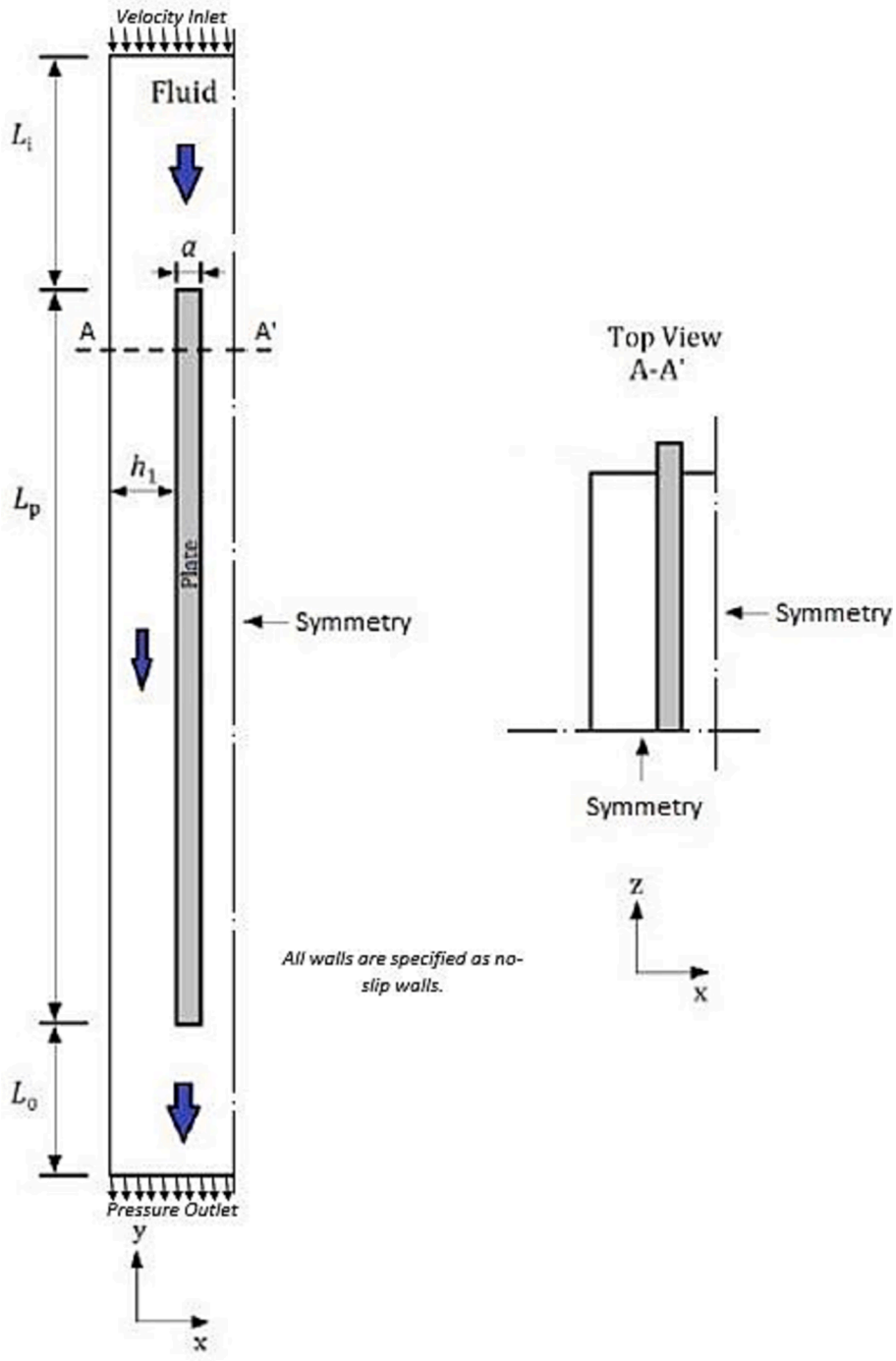

Fig. 2. Generic diagram of the computational domain. Source: (Mantecón, 2019) (Adapted).

- Nuclear Safety: Determining the critical flow velocity is essential for establishing safe operating limits for reactors. Therefore, the results of this research can be directly applied to ensure the safe operation of nuclear reactors, minimizing risks associated with mechanical problems in fuel elements.

2. Multiphysics analysis

FSI simulations can be classified as coupled in one way (unidirectional), or in two ways (bidirectional). In the unidirectional approach, only the pressure and friction forces obtained from the CFD analysis are transferred to the structural model. In the two-way approach, not only are fluid forces transferred to the structure, but the fluid domain is also updated as a result of structural deformations, in an iterative process, until both solutions reach a predefined convergence criterion.

In the current study, the simulation strategy employed was the partitioned method (Piperno et al., 1995), where the fluid and structure subproblems are solved iteratively. This strategy requires the use of two codes: one to solve the fluid dynamics equations, which in the present case was ANSYS – CFX Premium (ANSYS and Inc., 2021, 2021); and another for the structural part, for which we used ANSYS Mechanical Enterprise (ANSYS and Inc., 2021, 2021). For the coupling of the models, the ANSYS System Coupling module was used, with an implicit approach of bidirectional fluid–structure interaction, in steady state.

Table 1
Geometric specification of the computational domain.

Parameter	Dimension [mm]
Channel thickness,h	2.45
Channel width,b	70.5
Plates lengths,L_p	655
Plates thickness,a	1.35
Plates width,d	75
Inlet plenum,L_i	190
Outlet plenum,L_o	70

3. Numerical methodology

The numerical methodology used in this study was a simplification of the one presented by Javier Mantecón (Mantecón, 2019; Mantecón and Mattar Neto, 2018; Mantecón and Mattar Neto, 2019) to predict the onset of instability in fuel plates; however, employing a permanent regime. In this work, the turbulence and discretization model in the boundary layer region was also changed.

The computational domain studied was based on the geometric and hydraulic characteristics of the RMB fuel element (Fig. 1). The RMB fuel element has a square cross-section and is formed by assembling 21 flat-plate type fuel elements with a meat made of low-enrichment Uranium-Aluminum Silicide ($U_3Si_2 - Al$) dispersion coated with Aluminum (Perrotta and Soares, 2015). For the RMB fuel element, two types of fuel plates are provided, internal and external. The two external fuel plates 1a and 21a have a thicker coating, in order to provide greater structural rigidity to the set. In this study, the model is representative of the inner portion of the fuel element. Thus, its dimensions correspond to those of the inner plates.

In the present study, the flow is analyzed in a domain composed of an arrangement of two plates and three equal flow channels. However, only half of a plate was effectively modeled, since, taking advantage of geometric and loading symmetry, symmetry boundary conditions were applied and the computational domain used corresponds to 1/4 of that analyzed by Mantecón (Mantecón, 2019; Mantecón and Mattar Neto, 2018). With this simplified approach, it is possible to analyze the influence of neighboring fuel plates, and also extrapolate conclusions for sets of fuel elements composed of multiple plates. The generic domain diagram is shown in Fig. 2. In this, the blue arrows indicate the flow direction. The geometric specifications of the domain are summarized in Table 1.

3.1. Fluid model

Computational fluid analysis was performed using Reynolds-averaged Navier–Stokes equations (RANS), and the fluid domain was modeled using ANSYS CFX in a steady state condition. The model consists of an inlet plenum, cooling channels, and an outlet plenum (Fig. 2).

The boundary conditions were created in order to take advantage of the existing loading and geometric symmetry, and in the current study this allowed the use of a model corresponding to half of a plate. At the entrance to the domain, a velocity inlet boundary condition with a uniformly distributed profile in the y-axis direction was defined, as well as turbulence levels of 5 %. A least we know approximately the turbulence level at the inlet, this turbulence level is defined by the solver as

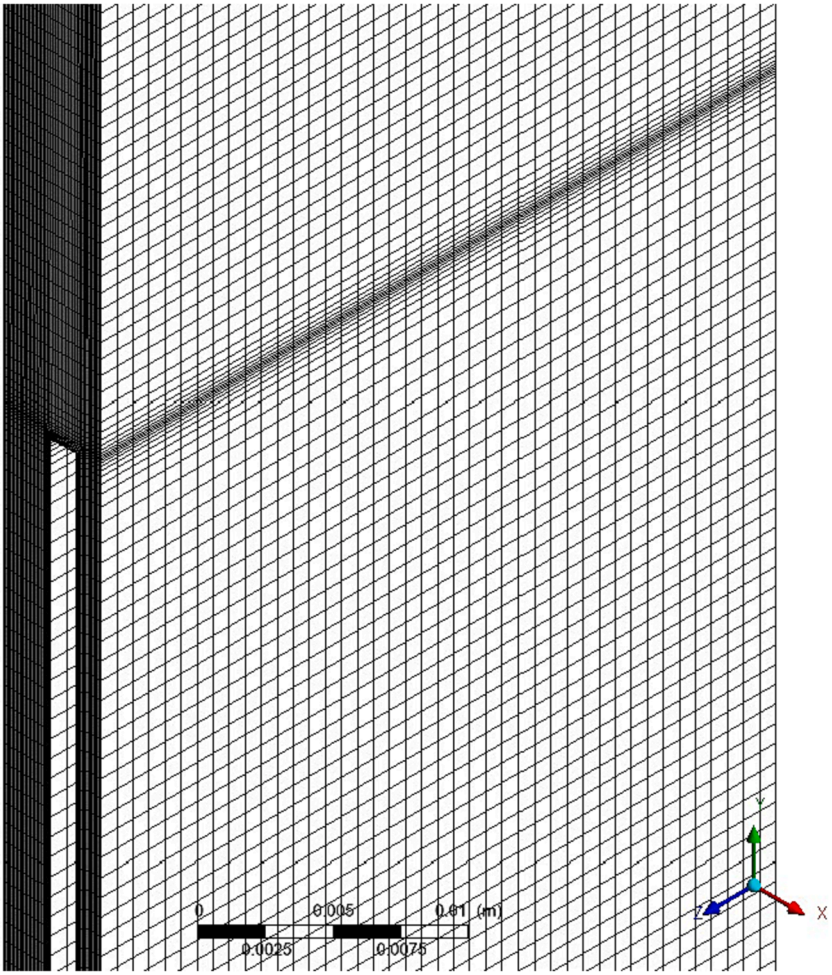

Fig. 3. Example of a mesh (F4) used in the CFD model.

the average value; and, unless it is known approximately the turbulence level at the inlet, it is the most recommended option. The inlet velocity was varied so that a set of flows was covered, that started with a velocity of 8.2 m/s in the channel, which is the minimum coolant velocity required in the RMB fuel element channels, up to a value of 17.68 m/s, higher than that calculated analytically through Miller's expression. The upstream boundary was positioned at a distance L_i from the leading edge of the plate. The downstream boundary, placed L_o downstream of the trailing edge, was modeled using a pressure output boundary condition with 0 Pa gage pressure. The fluid surfaces in contact with the plates were assumed to be deformable walls and with a no-slip condition. The boundary condition of a rigid and non-slip wall was imposed on the other external surfaces of the domain, with the exception of the two existing planes of symmetry.

For the generation of meshes of the fluid domain, ANSYS ICEM was used to generate hexahedral meshes. In order to verify the effect of completely solving the boundary layer and its result in the determination of the critical flow velocity, meshes with sufficient discretization to solve the entire boundary layer (herein named as Case 1) were studied, as well as meshes that model the boundary layer (i.e., mesh from the logarithmic layer - herein named as Case 2). In all cases, prism layers were used to properly capture the fuel plate boundary layer, and the height of the first cell was calculated to have the proper y^+ (Equation (2), which is a dimensionless parameter that relates the product of the friction velocity (u_τ) and the distance (y) to the nearest wall divided by the kinematic viscosity (ν).

$$y^+ = \frac{y u_\tau}{\nu} \tag{2}$$

u_τ can be defined in terms of shear stress τ_w and density ρ, that is:

$$u_\tau = \sqrt{\frac{\tau_w}{\rho}} \tag{3}$$

Fig. 3 shows the view of one of the meshes used in the region close to the leading edge.

Following the best practices recommended by the ASME V&V 20–2009 (Asme, 2009), a mesh convergence study was carried out, as described below, both for the fluid model and the structural model, in order to estimate numerical uncertainties due to discretization.

To numerically solve the unstable turbulent flow, the $\kappa-\omega$ SST (Shear- Stress-Transport) turbulence model was adopted. This turbulence model combines the best properties of the $\kappa-\epsilon$ and $\kappa-\omega$ (Menter, 1994) models, mixing the robust and accurate formulation of the $\kappa-\omega$ near-wall model, with the best formulation of the model $\kappa-\epsilon$ in the free stream. Thus, for low values of y^+, the model resolves the boundary layer from its viscous sublayer; and for values of y^+ greater than 30, the model uses wall functions. Finally, a root mean square (RMS) residual target of 10^{-6} as a convergence criterion and the stability of maximum plate pressure were considered.

3.1.1. Fluid model verification

ASME V&V 20–2009 (Asme, 2009) recommends the Grid Convergence Index (GCI) for estimating uncertainties due to discretization. The GCI method was developed by Roache (Roache, 1998) and provides an estimate of the discretization error by comparing results obtained by successive mesh refinements. The theoretical basis of the method is to assume that the solutions converge asymptotically to the exact solution as the number of elements is increased, with an apparent order of convergence theoretically proportional to the order of the discretization scheme.

In order to obtain good results using GCI, practical experience (Roache, 1998) has shown that mesh refinement ratios only need to be greater than 1.3. Thus, for three-dimensional meshes, the representative mesh size (h) can be calculated as follows:

Table 2
Water properties at 24 °C.

Property	Value
Dynamic viscosity, μ [$Pa.s$]	$8.87\text{x}10^{-4}$
Density, ρ[kg/m^3]	997.56

$$h = \left[\frac{1}{N}\sum_{i=1}^{N}\Delta V_i\right]^{\frac{1}{3}} \tag{4}$$

where ΔV_i is the volume of the ith element, and N is the total number of mesh elements. The mesh refinement factor is $r = h_{coarse}/h_{medium}$ or $r = h_{medium}/h_{fine}$.

Considering three distinct meshes (coarse − 3, medium − 2, fine − 1), a variable of interest (ϕ) is selected, and simulations are performed to determine the value of the key variable important for the simulation study objective.

Given $r_{21} = h_2/h_1$ and $r_{32} = h_3/h_2$, the apparent (or observed) order p (Eq. (5) of the method is calculated.

$$p = \left[\frac{1}{ln(r_{21})}\right]\left[ln\left|\frac{\phi_3-\phi_2}{\phi_2-\phi_1}\right| + q(p)\right] \tag{5}$$

$$q(p) = ln\left(\frac{r_{21}^p - s}{r_{32}^p - s}\right) \tag{6}$$

$$s = 1 \bullet sign\left(\frac{\phi_3-\phi_2}{\phi_2-\phi_1}\right) \tag{7}$$

Note that $q(p) = 0$ for constant r. This set of three equations can be solved through an iterative procedure, with the initial guess equal to the first term.

Next, the extrapolated value of the variable of interest ϕ_{ext}^{21} (Eq. (8) is calculated, along with the estimated relative error e_a^{21} (Eq. (9):

$$\phi_{ext}^{21} = \frac{r_{21}^p\phi_1 - \phi_2}{r_{21}^p - 1} \tag{8}$$

$$e_a^{21} = \left|\frac{\phi_1-\phi_2}{\phi_1}\right| \tag{9}$$

Finally, the Grid Convergence Index (GCI) for the finest mesh is calculated using Eq. (10).

$$GCI_{21} = \frac{F_s \bullet e_a^{21}}{r_{21}^p - 1} \tag{10}$$

In Eq. (10), the term F_s is the Factor of Safety; and, in the present study, the value of 1.25 was assigned to the F_s, which results in a GCI with a 95 % confidence interval. The value of $F_s = 1.25$ was recommended by Roache after conducting empirical studies, which were subsequently supported by several additional experiments in hundreds of CFD cases (Asme, 2009; Roache, 1998).

It is necessary to emphasize that there was no case of oscillatory convergence in the present work. All results showed monotonic convergence, and therefore, the previously presented equations were used. For cases where non-monotonic convergence is observed, ASME recommends a least-squares approach developed in the references (Eça and Hoekstra, 2002; Eça et al., 2005; Pelletier and Roache, 2000).

Thus, applying the CGI to the fluid domain, three progressively refined hexahedral meshes were run for Case 1, as well as for Case 2.

In all cases, the coolant considered was water with constant physical properties (see Table 2.), and the simulations were conducted in steady state. At the entrance to the fluid domain, a uniform fluid velocity was assumed and calculated so as to obtain a fluid velocity of 8.2 m/s in the channels, which is the minimum coolant velocity required in the RMB fuel assembly.

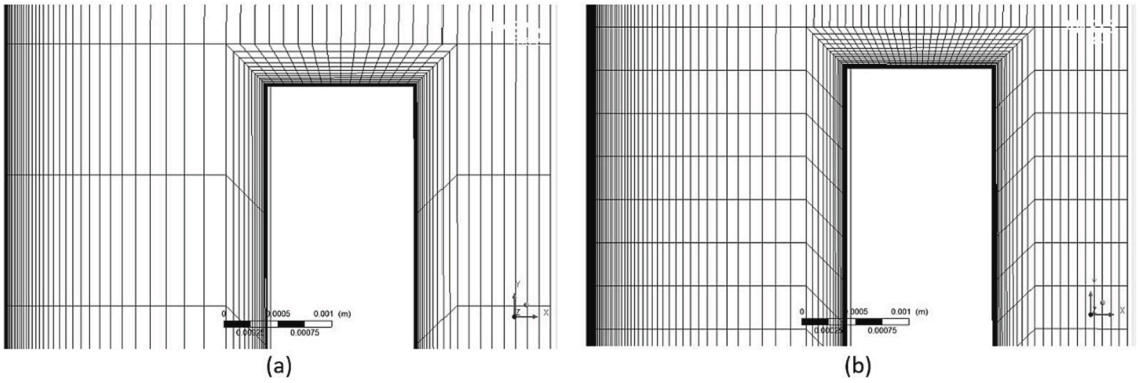

Fig. 4. Examples of meshes used in the fluid domain verification: (a) F3 mesh and (b) F1 mesh.

Table 3
Characteristics of the meshes used in the verification study and values of the key parameters for Case 1.

Mesh	Interior (cells)	h [mm]	r	P_{max} [Pa]	τ_w [Pa]	y^+
F1	12,385,850	0.3484	1.423	138886.00	195.44	0.51
F2	4,295,040	0.4958	1.428	137350.00	192.07	1.01
F3	1,474,950	0.7081	–	135264.00	189.91	1.50

Table 4
Characteristics of the meshes used in the verification study and values of the key parameters for Case 2.

Mesh	Interior (cells)	h [mm]	r	P_{max} [Pa]	τ_w [Pa]	y^+
F4	1,941,240	0.6461	1.307	135564.00	189.27	34.71
F5	869,430	0.8445	1.314	134172.00	187.04	39.87
F6	383,000	1.1099	–	133358.00	184.34	41.11

Table 5
Numerical uncertainty of the CFD domain - Case 1.

Parameter	ϕ_{ext}^{21} [Pa]	e_a^{21} [%]	GCI_{21} [%]
P_{max}	143373.5948	1.1059	4.0389
τ_w	186.1857	1.7243	5.9189

Table 6
Numerical uncertainty of the CFD domain - Case 2.

Parameter	ϕ_{ext}^{21} [Pa]	e_a^{21} [%]	GCI_{21} [%]
P_{max}	132281.2046	1.0268	3.0270
τ_w	201.3682	1.1782	7.9900

In the GCI application, the maximum pressure (P_{max}) and the shear stress on the surface of the plates (τ_w) were selected as the key parameters to evaluate the uncertainties.

Fig. 4 shows examples of the meshes used in the verification of the fluid model, with sufficient discretization to resolve the boundary layer (Case 1).

In this figure, mesh (a) is the mesh referred to here as F3; and (b) is the F1 mesh. Table 3 presents the details of the three meshes used in the convergence study for Case 1, where the finest mesh is identified as mesh F1. Table 4 shows the same data, but for the meshes of Case 2.

Finally, tables 5 and 6 present the numerical uncertainty results reported for grids F1 and F4 respectively.

The results of the uncertainty studies presented for the fluid domain show that: 1) for Case 1, there was a maximum uncertainty of around 5.9 %, already working with the maximum computational capacity available, which prevents further refinements to try to reduce this uncertainty; for Case 2, the highest reported uncertainty was in the order of 7.9 %. However, analyzing the obtained values, it is noticed that, in absolute values, the parameters vary very little. This leads us to believe that the models are reliable, and so it was decided to continue the study with the F1 and F4 meshes.

Table 7
Aluminum alloy 6061-T6 properties at a temperature of 24 °C.

Property	Value
Density, ρ_m [kg/m^3]	2700
Poisson's ratio,ν	0.33
Young's modulus, E [GPa]	68.9
Yield strength, σ_y [MPa]	276

3.1.2. Structural model

For the solid domain, aluminum alloy 6061-T6 was considered as the plate material. The properties of this material are shown in Table 7..

For the modeling of the structural part of the multiphysics domain, we used ANSYS Mechanical Enterprise in the static analysis. The fuel plate was discretized using a structured mesh with SOLID186 hexahedral elements, produced using ANSYS Meshing. Along one of the sides parallel to the flow, a region of 2.25 mm of the width of the plate was used to fix it, and the boundary condition imposed was a restriction on the displacements at X = y = z = 0. On the other side, parallel to the flow, the symmetry boundary condition was applied. On the surfaces of the plate in contact with the fluid, a fluid–solid interface boundary condition was specified. This interface is where the data resulting from each module is transferred bidirectionally. The leading and trailing edges of the plate are free.

3.1.3. Solid model verification

A mesh convergence test was also completed to verify the solid model. For this, three different meshes were also generated, and static analyses were performed using the Static Structural module of ANSYS Mechanical. The same boundary condition, as previously described, was used to fix the plate on one of its surfaces parallel to the flow. On one of the faces of the plate, a uniform pressure load (P) was applied. This

Table 8
Characteristics of the meshes used in the solid domain verification study and key parameter values.

Mesh	Interior (cells)	h [mm]	r	δ_m [mm]
E1	74,800	0.9607	1.3116	138886.00
E2	33,150	1.2600	1.3168	137350.00
E3	14,520	1.6592	–	135264.00

Table 9
Numerical uncertainty of the solid domain.

Parameter	$\phi_{ext}^{21}[mm]$	$e_a^{21}[\%]$	$GCI_{21}[\%]$
δ_m	0.5792	0.1038	0.2040

Table 10
Velocities simulated in this work.

Simulation	$v_o[m/s]$	$v_{in}[m/s]$
1	8.20	6.00
2	9.26	6.77
3	10.10	7.39
4	10.95	8.01
5	11.79	8.62
6	12.63	9.24
7	13.47	9.85
8	14.31	10.47
9	15.16	11.08
10	16.00	11.70
11	16.84	12.32
12	17.68	12.93

pressure is equal to the maximum pressure found with the F1 mesh in the fluid model verification subsection, in order to simulate the hydraulic pressure head to which the plates are exposed when coupled to the fluid domain. In the position corresponding to half the width of the plate, the condition of symmetry along its longitudinal direction (XY plane) was applied.

Again, we applied the GCI method to estimate uncertainties. As a key parameter, the deflection at the midpoint (δ_m) was chosen. Table 8 presents the characteristics of the meshes and the values obtained for the selected parameter. Finally, Table 9. presents the uncertainty quantification of the structural model and, as can be seen, the uncertainty obtained for mesh E1 is very low, confirming that this mesh is suitable for the study.

4. Results and discussion

Using Eq. (1), we calculated the value of the Miller velocity of the RMB fuel element assembly and obtained the value of 16.84 m/s, which is consistent with the one reported by (de Oliveira, 2011) (16.86 m/s).

The FSI simulations were carried out for the set of flows presented in Table 10. These input velocities were selected in order to obtain a velocity in the channel ranging from 8.2 m/s to 17.68 m/s. All simulations were carried out until the convergence criteria were reached, namely: residuals of all conservation equations 10^{-6}, global variables stable throughout the iterations, and residual target of mesh displacement less than 0.5 %.

4.1. Case 1 results

Fig. 5 shows the velocity magnitude contours near the leading edge of the fuel element plates, in the mid-plane of the cooling channels.

For post-processing, line probes were created along the axial centerline of the fuel element plate, and total mesh displacements were obtained. Fig. 6 presents an example of this axial centerline, which extends from the leading edge to the trailing edge, used in Case 1. It should be mentioned that this image was generated using the symmetry expansion feature available in ANSYS. From these displacements, it was possible to generate the static deflection profile of the fuel plate, as shown in Fig. 7.

The profile obtained is coherent with what was expected, showing an increase in deflection due to the increase in flow. It is also noted that, for all speeds, the greatest deflection occurred at the leading edge of the plate. Furthermore, for the highest velocity, it is possible to notice an increase in deflection near the trailing edge of the plate, a phenomenon that has already been captured by other authors (Kennedy, 2015; Mantecón, 2019; Mantecón and Mattar Neto, 2018; Mantecón and Mattar Neto, 2019).

Fig. 8 presents the contour plots of plate deflection for different flow velocities. In these images, the ANSYS symmetry expansion resource was used again, in order to present a complete plate. Remembering that we modeled the combustible element plate on the left, and used the symmetry condition, we verified that the boundary condition is well placed, since the phenomenon of displacements of the adjacent plates in opposite directions was correctly captured. It was also verified that, in addition to the static divergence at the leading edge, the plate can suffer deflections along its length.

Mantecón (Mantecón, 2019; Mantecón and Mattar Neto, 2018; Mantecón and Mattar Neto, 2019) observed that the dynamic pressure of the fluid on the plate is proportional to the square of the velocity of the fluid, and, based on this observation, proposed a methodology to

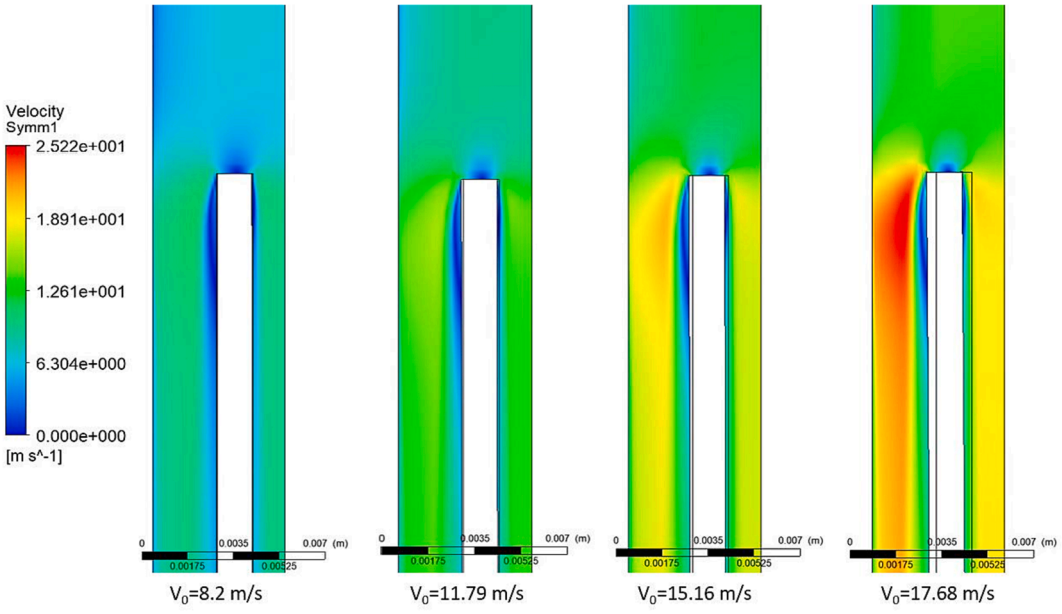

Fig. 5. Velocity contours along the mid-plane of the channels and close to the leading edge of the plates for several fluid velocities.

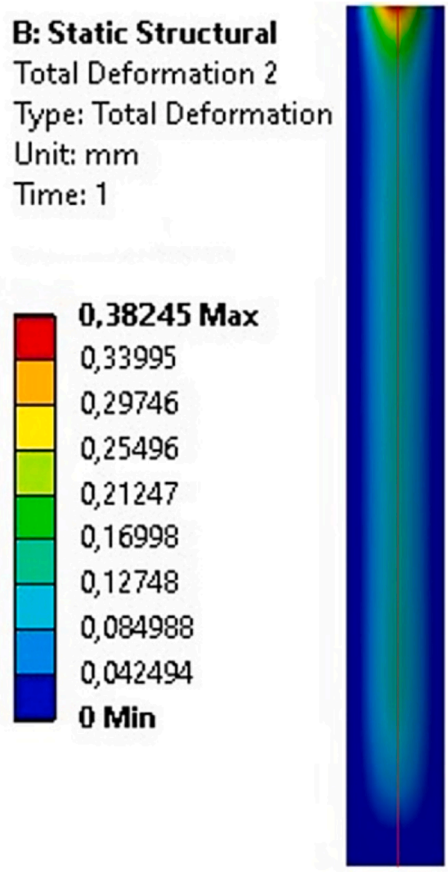

Fig. 6. Centerline used for extracting the axial deflection profile of the plates (in this case $v_0 = 17.68$ m/s).

numerically predict the critical flow velocity. Plotting the maximum plate deflection and the square of the mean velocity of the coolant in the channels, the aforementioned author noted that it was possible to perceive two trends in the data presented: for lower velocities, it was noted that the maximum plate deflection is a linear function of the square of the velocity of the fluid in the channels; however, after a certain value, it was noticed that the deflection increases more quickly and that the behavior no longer maintains a linear trend. This point then, is where the critical speed is identified.

Therefore, analyzing Fig. 9, it can be identified that the critical velocity obtained for Case 1 is 15.16 m/s, and the maximum deflection of the plate at this velocity is $\delta_{Case1} = 0.1572$ mm.

4.2. Case 2 results

In Case 2, where the wall law was used to model the boundary layer, the same criterion as the previous subsection was applied to identify the critical velocity; that is, the speed at which the maximum plate deflection changes from linear to non-linear behavior. In this way, analyzing Fig. 10, which presents the maximum deflection of the plate versus the velocity squared, it is possible to identify that the velocity of the fluid where the shape of the curve was changed is equal to 15.16 m/s; that is, the same as identified for Case 1.

4.3. Comparison with Miller velocity

Following the trend initiated by Zabriskie (Zabriskie, 1958; Zabriskie, 1959), a possible comparison to be made is to relate the critical velocity obtained in this research with the critical velocity calculated analytically through the Miller formula (Equation (1). Therefore, by dividing the value obtained in Cases 1 and 2 ($V_c = 15.16$ m/s) by the analytically calculated value ($V_M = 16.84$ m/s), it can be seen that the numerically obtained value 10 % below the Miller velocity. Thus, it is noted that the value obtained numerically is more conservative than the one calculated by the Miller formula.

Superimposing the results of maximum deflection of the plate as a function of the square of the velocity of Cases 1 and 2 (Fig. 11), the

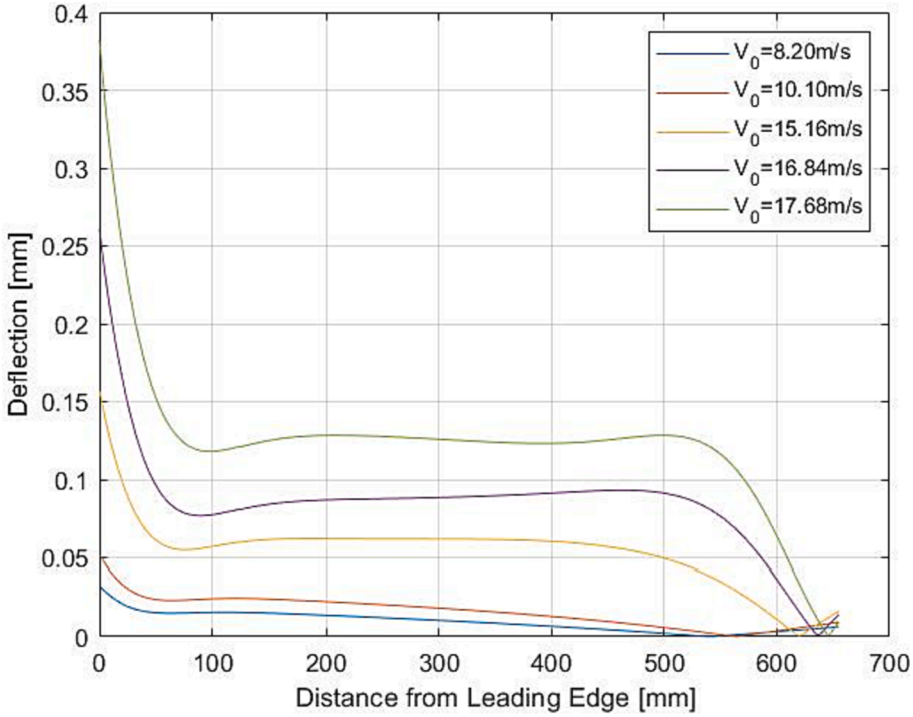

Fig. 7. Plate deflection profile for different flow velocities - mesh E1.

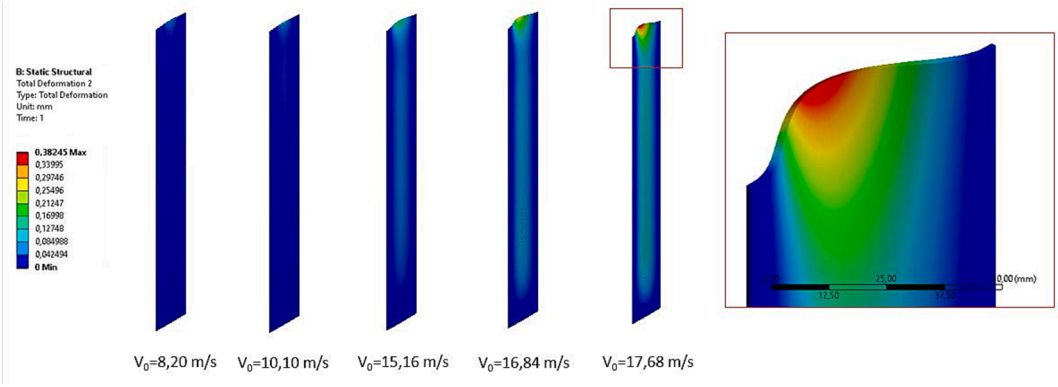

Fig. 8. Plate deflection contours for different fluid velocities. Flow in the -y direction. Deflection scale factor of 43x.

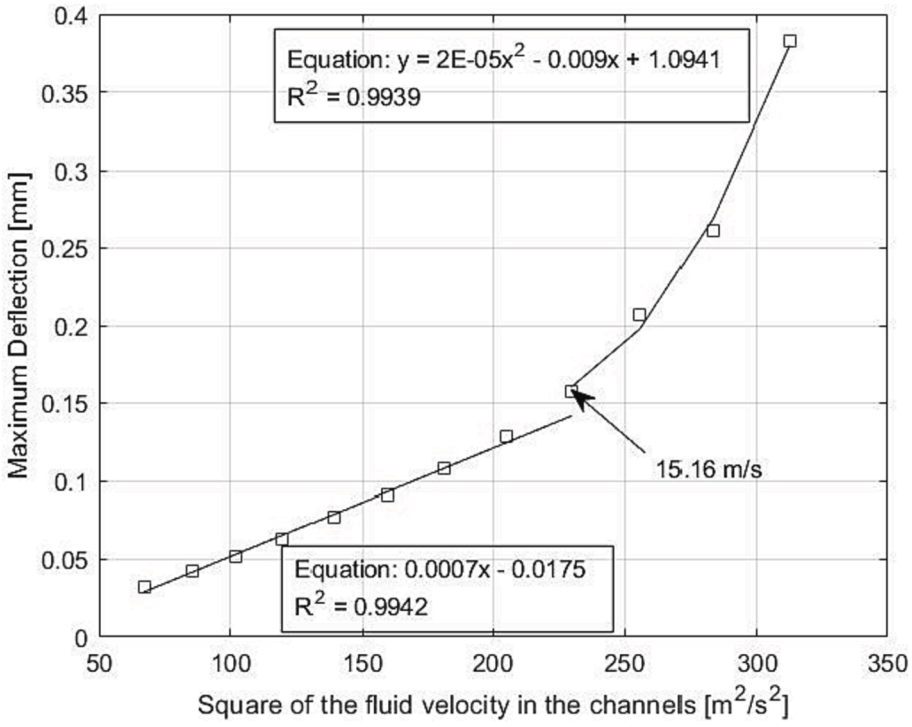

Fig. 9. Maximum plate deflection as a function of the square of the velocity in the channel - Case 1.

overlapping of results up to the velocity of 14.31 m/s can be verified. From the critical velocity found (V_c), differences in the obtained deflections begin to appear, reaching a maximum difference of around 6 % for the highest velocity.

4.4. Comparison with previous studies related to the RMB

As part of the development of the RMB, numerical simulations (Mantecón, 2019; Mantecón and Mattar Neto, 2018) have already been carried out in order to identify the critical speed. Fig. 12 was published by Mantecón, on which it can be seen that the value obtained in the study was 16.84 m/s, exactly coinciding with Miller's formula, and the maximum deflection found at this speed was $\delta_{Mantecon} = 0.1252$ mm.

It is noteworthy that, although the critical velocity numerically obtained by Mantecón is greater than that obtained in the present research, the maximum deformation found by the author in the leading edge of the plate is approximately 20 % smaller than that found in the critical velocity of Case 1.

5. Conclusions

In the current work, the contribution of viscous effects on the mechanical stability of nuclear fuel plates under axial flow conditions was investigated, applying the methodology proposed by Javier Mantecón (Mantecón, 2019; Mantecón and Mattar Neto, 2018); however, in a permanent regime. The model adopted is representative of the fuel plates and cooling channels designed for the RMB. The numerical strategy was based on the bidirectional fluid–structure interaction method. The important results of the current study can be summarized as follows:

- The methodology managed to capture the phenomenon well for Cases 1 and 2, suggesting that steady state and static modeling are feasible. This approach, as well as the application of symmetry boundary conditions, allow a significant saving of computational power;
- The results obtained in this work to characterize the instability in the plates are 10 % lower than those reported using the transient and

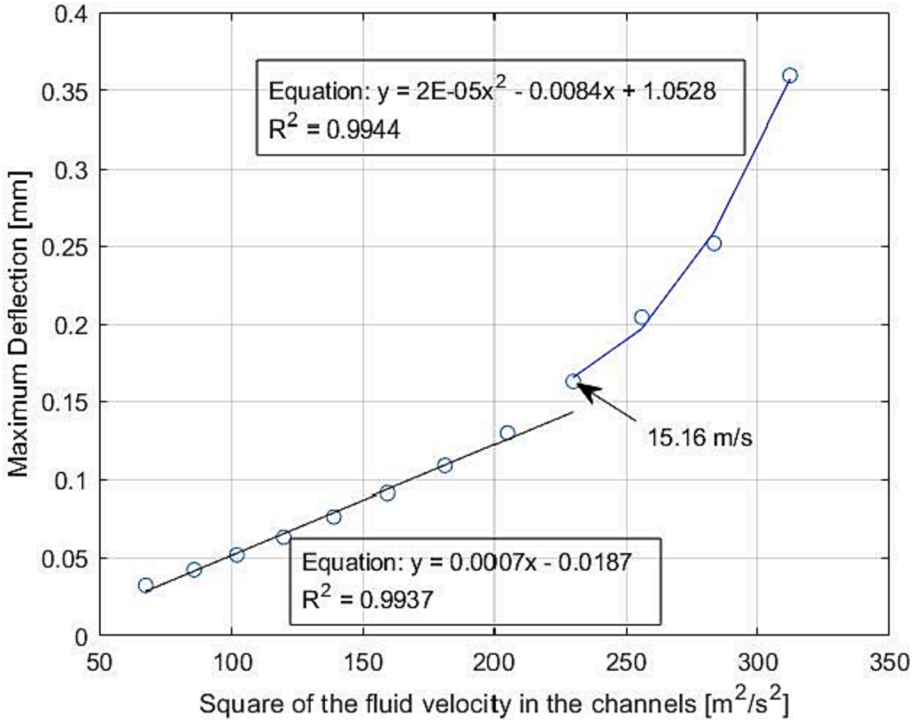

Fig. 10. Maximum plate deflection as a function of the square of the velocity in the channel - Case 2.

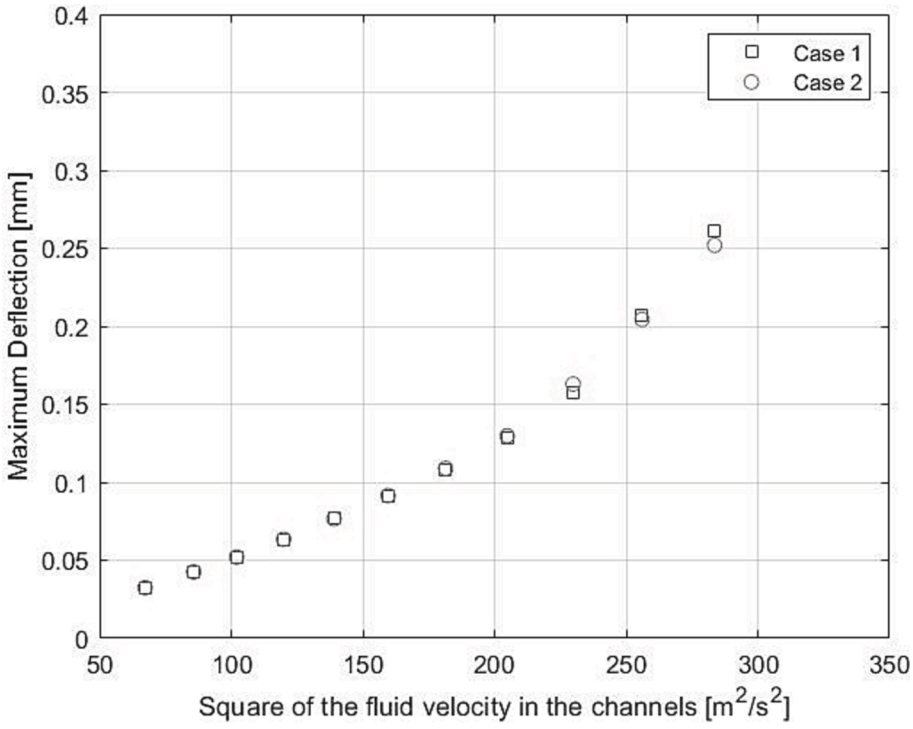

Fig. 11. Comparison of the maximum plate deflection as a function of the square of the velocity in the channel.

dynamic regime modeling performed by Mantecón (Mantecón, 2019; Mantecón and Mattar Neto, 2018);

- The value of the critical velocity obtained numerically in this research corresponds to 90 % of that calculated by the Miller formula, thus being more conservative than this one;
- The results of cases 1 and 2 showed that the maximum deflection was detected at the leading edge; and, the comparison of the results revealed that the complete resolving of the boundary layer from its viscous sublayer are not relevant for the determination of the critical velocity; and
- During all analyses, the fuel plates did not undergo an abrupt or catastrophic collapse at any speed, and no plastic deformation was noted.

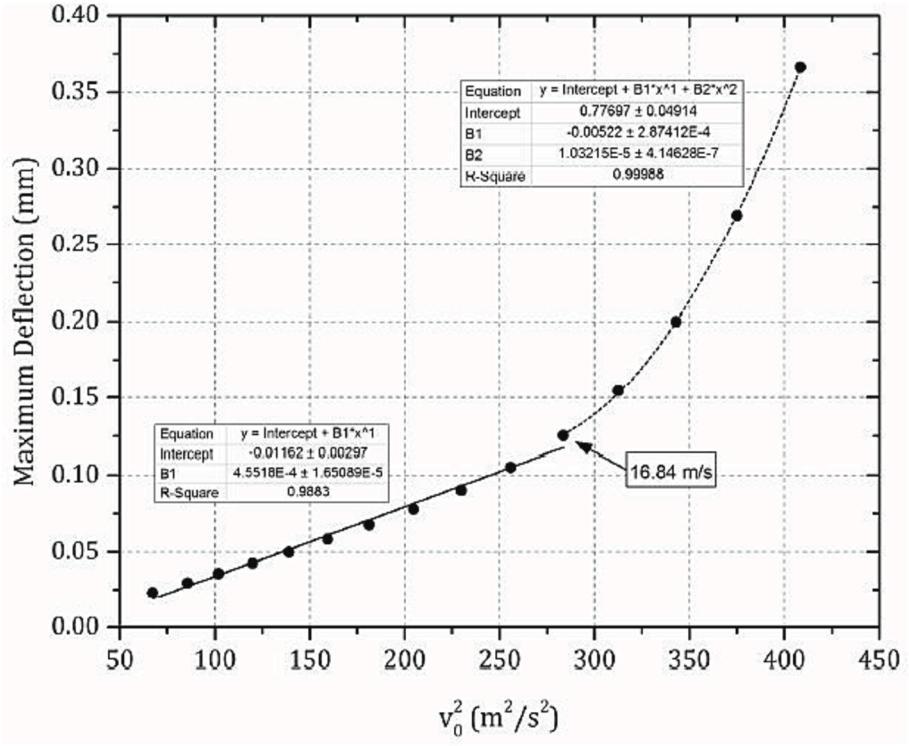

Fig. 12. Critical velocity obtained by Mantecón. ().
Source: Mantecón, 2019

It can be concluded, therefore, that the main contribution of the present research is that we proved that boundary layer modeling is sufficient to study the critical velocity of plate-type fuel elements. The results obtained here also suggest that numerical simulations of fluid–structure interactions can be carried out at steady state and with the application of symmetry-type boundary conditions, where possible. This approach results in significant savings in time and computational resources, and can be used during the design of new fuel sets, supporting traditional methods. Once again, it is emphasized that the research is closely related to nuclear reactor technology, aiming to enhance the safety and efficiency of these systems through the study of fluid–structure interaction.

This research did not receive any specific grant from funding agencies in the public, commercial, or not-for-profit sectors.

CRediT authorship contribution statement

A.J.S. Moura: Methodology, Formal analysis, Investigation, Writing – original draft, Visualization. **M. Mattar Neto:** Conceptualization, Resources, Writing – review & editing, Supervision, Project administration.

Declaration of Competing Interest

The authors declare that they have no known competing financial interests or personal relationships that could have appeared to influence the work reported in this paper.

Data availability

Data will be made available on request.

References

ANSYS Inc. Ansys CFX Reference Guide - Release 2021 R2, 2021.
ANSYS Inc. Ansys Mechanical User's Guide - Release 2021 R2, 2021.
Asme, 2009. Standard for Verification and Validation in Computational Fluid Dynamics and Heat Transfer. Normes ASME. American Society of Mechanical Engineers.
Bang, C.S., Rana, Z.A., Könözsy, L., Marchante Rodriguez, V., Temple, C., 2022. Numerical investigation and fluid-structure interaction (fsi) analysis on a double-element simplified formula one (f1) composite wing in the presence of ground effect. Fluids 7 (2), 85.
Cekirge, H., Ural, E., 1978. Critical coolant flow velocities in reactors having parallel fuel plates. Comput. Math. Appl. 4 (2), 153–156.
Curtis, F. G., Ekici, K., and Freels, J. D. Fluid-Structure Interaction Modeling of High-Aspect Ratio Nuclear Fuel Plates Using COMSOL. In COMSOL Multiphysics Conference (2013).
Curtis, F.G., Freels, J.D., Ekici, K., 2018. Predicting large deflections of multiplate fuel elements using a monolithic fsi approach. Nucl. Sci. Eng. 189 (1), 82–92.
Curtis, F.G., Freels, J.D., Ekici, K., 2019. Deflection predictions of involute-shaped fuel plates using a fully-coupled numerical approach. Ann. Nucl. Energy 130, 184–191.
Davis, D., and Kim, G. Design Against Hydrodynamic Instabilities in Flat-Plate Type Fuel Element Assemblies. (1991).
Davis, D.C., Scarton, H.A., 1985. Flow-induced plastic collapse of stacked fuel plates. Nucl. Eng. Des. 85 (2), 193–200.
C.A. de Oliveira M. Mattar Neto Flow velocity calculation to avoid instability in a typical research reactor core, In, International Nuclear Atlantic Conference Belo Horizonte, Brazil 2011 2011 1 6.
de Sa Andrzejewski, C. Estudo da deposição termoforética de partículas na fabricação de fibras óticas, 2005.
Eça, L., and Hoekstra, M. An evaluation of verification procedures for CFD applications, 2002.
Eça, L., Hoekstra, M., and Roache, P. Verification of calculations: An overview of the 2nd Lisbon workshop, 2005.
El-Wakil, M.M., 1962. Nuclear Power Engineering. McGraw-Hill Compa-nies.
Glasstone, S., Sesonske, A., 2012. Nuclear reactor engineering: reactor systems engineering. Springer Science & Business Media.
González Mantecón, J., Mattar Neto, M., 2020. Numerical investigation on the effects of geometric deviations and materials properties on flow-induced deflections of fuel plates. Ann. Nucl. Energy 140.
Groninger, R.D., Kane, J.J., 1963. Flow induced deflections of parallel flat plates. Nucl. Sci. Eng. 16 (2), 218–226.
C. Guo M. Païdoussis Analysis of Hydroelastic Instabilities of Rectangular Parallel-Plate Assemblies Journal of Pressure Vessel Technology 122, 4 (03 2000), 502 508.
Howard, T., Marcum, W., Jones, W., 2015. A novel approach to modeling plate deformations in fluid-structure interactions. Nucl. Eng. Des. 293, 1–15.
Jensen, P., Marcum, W., 2014. Predicting critical flow velocity leading to laminate plate collapse-flat plates. Nucl. Eng. Des. 267, 71–87.
Jensen, P. J. Application of sandwich structure analysis in predicting critical flow velocity for a laminated flat plate. 2013.
Jesse, C.J., 2015. Analysis of the potential for flow-induced deflection of nuclear reactor fuel plates under high velocity flows. University of Missouri-Columbia.

E.B. Johansson Hydraulic instability of reactor parallel-plate fuel assemblies 1959 Knolls Atomic Power Laboratory Schenectady, USA Report No. KAPL-M-EJ-9.
Kaufmann, A.R., 1962. Nuclear Reactor Fuel Elements: Metallurgy and Fabrication. Interscience Publishers.
Kennedy, J.C., 2012. Hydro-mechanical analysis of low enriched uranium fuel plates for University of Missouri Research Reactor. University of Missouri-Columbia. PhD thesis,.
Kennedy, J.C., 2015. Development and experimental benchmarking of numeric fluid structure interaction models for research reactor fuel analysis. University of Missouri-Columbia.
Kim, G., Davis, D., 1995. Hydrodynamic instabilities in flat-plate-type fuel assemblies. Nucl. Eng. Des. 158 (1), 1–17.
Li, Y., Lu, D., Zhang, P., Liu, L., 2012. Experimental investigation on fluid-structure interaction phenomenon caused by the flow through double-plate structure in a narrow channel. Nucl. Eng. Des. 248, 66–71.
Mantecón, J.G., 2019. Evaluation of mechanical stability of nuclear fuel plates under axial flow conditions. Universidade de São Paulo. PhD thesis,.
Mantecón, J.G., Mattar Neto, M., 2018. Numerical methodology for fluid-structure interaction analysis of nuclear fuel plates under axial flow conditions. Nucl. Eng. Des. 333, 76–86.
Mantecón, J.G., Mattar Neto, M., 2019. Numerical analysis on stability of nuclear fuel plates with inlet support comb. Nucl. Eng. Des. 342, 240–248.
Menter, F.R., 1994. Two-equation eddy-viscosity turbulence models for engineering applications. AIAA J. 32 (8), 1598–1605.
Miller, D.R., 1958. Critical Flow Velocities for Collapse of Reactor Parallel-Plate Fuel Assemblies. Knolls Atomic Power Laboratory, Schenectady. Report No. KAPL-1954,.
Pavone, S.J., Scarton, H.A., 1983. Laminar flow induced deflections of stacked plates. Nucl. Eng. Des. 74 (1), 79–89.
Pelletier, D., Roache, P.J., 2000. Verification and Validation of Computational Heat Transfer ch. 13, 417–442.
Perrotta, J.A., Soares, A.J., 2015. RMB: the new brazilian multipurpose research reactor. Int. J. Nucl. Power 60, 30–34.
Piperno, S., Farhat, C., Larrouturou, B., 1995. Partitioned procedures for the transient solution of coupled aeroelastic problems part i: Model problem, theory and two-dimensional application. Comput. Methods Appl. Mech. Eng. 124 (1–2), 79–112.
R. Doan The Engineering Test Reactor – A Status Report. 16 1958 Nucleonics (US) Ceased publication.
R.L. Smith Dynamic Pressure Limits for Flat Plates as Related to Nuclear Fuel Elements 1968 Lewis Research Center Cleveland, USA Report No. NASA TN D-4417.
Roache, P., 1998. Verification and Validation in Computational Science and Engineering. Hermosa Publishers.
Scavuzzo, R.J., 1965. Hydraulic instability of flat parallel-plate assemblies. Nucl. Sci. Eng. 21 (4), 463–472.
Smissaert, G.E., 1968. Static and dynamic hydroelastic instabilities in MTR-type fuel elements Part I. Introduction and experimental investigation. Nucl. Eng. Des. 7 (6), 535–546.
Smissaert, G.E., 1969. Static and dynamic hydroelastic instabilities in MTR-type fuel elements part II. Theoretical investigation and discussion. Nucl. Eng. Des. 9 (1), 105–122.
Stromquist, W., and Sisman, O. High Flux Reactor Fuel Assemblies Vibration and Water Flow. Problem Assignment No. TX5-12. Tech. rep., Oak Ridge National Lab., Tenn., 1948.
Swinson, W., Battiste, R., Luttrell, L., Yahr, G., 1995. An ex-perimental investigation of the structural response of reactor fuel plates. Exp. Mech. 35, 212–215.
Swinson, W., Yahr, G., 1990. Dynamic pressure approach to analysis of reactor fuel plate stability. Oak Ridge National Lab. Tech. rep.,.
Wambsganss, M., 1967. Second-order effects as related to critical coolant flow velocities and reactor parallel plate fuel assemblies. Nucl. Eng. Des. 5 (3), 268–276.
Wang, Y., Bian, X., Wang, T., Huang, G., 2023. Numerical investigation of hydraulic instability of circular arc shell-type fuel elements under axial flow conditions. Nucl. Eng. Des. 405.
Wang, G., Bojanowski, C., Dave, A., Jaluvka, D., Hu, L.-W., Wilson, E., 2023. Numerical simulations of flow-induced deflections in mitr leu fuel plate due to channel size disparity. Nucl. Technol. 1–22.
D.S. Weaver T.E. Unny The Hydroelastic Stability of a Flat Plate Journal of Applied Mechanics 37, 3 (09 1970), 823 827.
Zabriskie, W.L., 1958. An Experimental Evaluation of Critical Flow Velocity Formulas for Parallel Plate Assemblies. Schenectady, USA.
Zabriskie, W.L., 1959. An Experimental Evaluation of the Effect of Length-to-Width Ratio on the Critical Flow Velocity of Single Plate Assemblies. Schenectady, USA.